THE JOURNAL OF BIOLOGICAL CHEMISTRY
Vol. 275, No. 25, Issue of June 23, pp. 18732–18738, 2000

Printed in U.S.A.

Inhibition of Calcium Release-activated Calcium Current by Rac/Cdc42-inactivating Clostridial Cytotoxins in RBL Cells*

Received for publication, February 22, 2000, and in revised form, March 31, 2000
Published, JBC Papers in Press, April 3, 2000, DOI 10.1074/jbc.M001425200

Nabil Djouder‡, Ulrike Prepens‡, Klaus Aktories‡§, and Adolfo Cavalié¶

From the ‡Institut für Pharmakologie und Toxikologie der Universität Freiburg, D-79104 Freiburg and the ¶Institut für Pharmakologie und Toxikologie der Universität des Saarlandes, D-66421 Homburg (Saar), Germany

Using large clostridial cytotoxins as tools, the role of Rho GTPases in activation of RBL 2H3 hm1 cells was studied. *Clostridium difficile* toxin B, which glucosylates Rho, Rac, and Cdc42 and *Clostridium sordellii* lethal toxin, which glucosylates Rac and Cdc42 but not Rho, inhibited the release of hexosaminidase from RBL cells mediated by the high affinity antigen receptor (FcεRI). Additionally, toxin B and lethal toxin inhibited the intracellular Ca^{2+} mobilization induced by FcεRI-stimulation and thapsigargin, mainly by reducing the influx of extracellular Ca^{2+}. In patch clamp recordings, toxin B and lethal toxin inhibited the calcium release-activated calcium current by about 45%. Calcium release-activated calcium current, the receptor-stimulated Ca^{2+} influx, and secretion were inhibited neither by the Rho-ADP-ribosylating C3-fusion toxin C2IN-C3 nor by the actin-ADP-ribosylating *Clostridium botulinum* C2 toxin. The data indicate that Rac and Cdc42 but not Rho are not only involved in late exocytosis events but are also involved in Ca^{2+} mobilization most likely by regulating the Ca^{2+} influx through calcium release-activated calcium channels activated via FcεRI receptor in RBL cells.

Cross-linking of the high affinity IgE receptor (FcεRI)[1] by antigen-binding induces a cascade of morphological and biochemical reactions, finally resulting in degranulation (1). Several signaling events have been described, which appear to be essential for FcεRI-mediated degranulation, including activation of protein tyrosine kinases and increase of intracellular Ca^{2+} (Refs. 2 and 3; for review, see Refs. 4 and 5). Activation of FcεRI leads to the stimulation of phospholipase Cγ and an increase of IP_3 levels, which depletes endoplasmic Ca^{2+} stores. Subsequently, a transient increase in the intracellular concentration of Ca^{2+} ($[Ca^{2+}]_i$) is followed by a sustained plateau which reflects the entry of extracellular Ca^{2+} (6). This Ca^{2+} entry is suggested to depend on the depletion of intracellular Ca^{2+} stores and is termed capacitative Ca^{2+} entry (for review, see Refs. 7 and 8). The inward Ca^{2+} current in RBL cells that seems to contribute to this entry is designated I_{CRAC} for calcium release-activated calcium current. However, the regulatory mechanisms leading to activation of I_{CRAC} is still unclear. Small GTPases have been suggested to participate in receptor-mediated Ca^{2+} influx in RBL cells and mast cells (9).

The small GTPases of the Rho family including Rho, Rac, and Cdc42 play important roles in regulation of the actin cytoskeleton (10). RhoA participates in growth factor-mediated formation of stress fibers and cell adhesions (11), Rac regulates membranes ruffling and lamellipodia (12), and Cdc42 controls the formation of filopodia (13). In addition, Rho GTPases participate as molecular switches in various signaling processes including regulation of phospholipase D (14), phospholipase $C\beta_2$ (15), phosphoinositide 3-kinase (16, 17), and phosphatidylinositol-4-phosphate 5-kinase (18). Furthermore, Rho subfamily proteins are involved in activation of transcription, cell cycle progression, and transformation (for review, see Refs. 10 and 19). The low molecular mass GTP-binding proteins of the Rho family (Rho, Rac, Cdc42) appear to be involved in activation of mast cells and RBL cells (20). Introduction of Rac into permeabilized mast cells cause secretion (21), and expression of dominant inhibitory forms of Cdc42 and Rac1 inhibits antigen-induced degranulation (22).

Recently, various bacterial toxins have been established as tools to study the function of small GTPases (23). *Clostridium botulinum* C3 transferase and related C3-like exoenzymes, including the C3 chimeric toxin C2IN-C3, selectively ADP-ribosylate RhoA, RhoB, and RhoC at Asn-41, thereby inhibiting their biological functions (24–27). The family of large clostridial cytotoxins inactivate small GTPases by glucosylation (28). Whereas *Clostridium difficile* toxins A and B monoglucosylate Rho GTPases including Rho, Rac, and Cdc42 at Thr-37 or Thr-35, respectively (29), the lethal toxin from *Clostridium sordellii* modifies Rac, possibly Cdc42, but not Rho (30, 31). In addition, Ras subfamily proteins (*e.g.* Ras, Ral, and Rap) are glucosylated by the lethal toxin.

Here we studied the effects of toxins on degranulation, Ca^{2+} mobilization, and I_{CRAC} in RBL 2H3 hm1 cells. We report that toxin B and lethal toxin but not the Rho-modifying chimeric toxin C2IN-C3 inhibit secretion and increase of $[Ca^{2+}]_i$ by the FcεRI receptor in RBL cells. Moreover, the toxins inhibit thapsigargin-induced Ca^{2+} mobilization and the activation of I_{CRAC} by depletion of intracellular Ca^{2+} stores, indicating that Rac/Cdc42 but not Rho participates in regulation of capacitative Ca^{2+} entry.

* This work was supported by grants from the Deutsche Forschungsgemeinschaft (to K. A. and A. C.) and a grant from the BMBF (clinical research group "Pathomechanismen der allergischen Entzündung" (to K. A.). The costs of publication of this article were defrayed in part by the payment of page charges. This article must therefore be hereby marked "*advertisement*" in accordance with 18 U.S.C. Section 1734 solely to indicate this fact.

§ To whom correspondence should be addressed: Inst. für Pharmakologie und Toxikologie, Albert-Ludwigs-Universität Freiburg, Hermann-Herder-Str. 5, D-79104 Freiburg, Germany. Tel.: 49-761-203-53-01; Fax: 49-761-203-53-11; E-mail: aktories@uni-freiburg.de.

[1] The abbreviations used are: FcεRI, high affinity receptor for IgE; C2 toxin, *C. botulinum* C2 toxin consisting of the enzyme component C2I and the binding component C2II; C2IN-C3, C3 fusion toxin consisting of C3 ADP-ribosyltransferase and the N-terminal part of component I of *C. botulinum* C2 toxin; $[Ca^{2+}]_i$, cytoplasmic free calcium; $[Ca^{2+}]_o$, extracellular free calcium; TNP-OVA, trinitrophenyl-conjugated ovalbumin; I_{CRAC}, calcium release-activated calcium current; IgE, immunoglobulin E; IP_3, inositol 1,4,5-triphosphate; lethal toxin, *C. sordellii* lethal toxin; PAGE, polyacrylamide gel electrophoresis; F, farad(s); PBS, phosphate-buffered saline.

EXPERIMENTAL PROCEDURES

Materials—*C. difficile* toxin B (32), *C. sordellii* lethal toxin (30), *C. botulinum* C2 toxin (33), and the C3 fusion toxin (C2IN-C3) (27) were prepared as described recently. Trinitrophenyl-ovalbumin (TNP-OVA) and IgE were kindly donated by Dr. A. Hoffmann (Paul-Ehrlich Institute, Langen, Germany). Fura-2 acetoxymethylester was obtained from Molecular Probes (Göttingen, Germany). Thapsigargin was obtained from Sigma and IP_3 from Calbiochem.

Cell Culture—Rat Basophilic Leukemia cells transfected with the human muscarinic receptor (34) (RBL 2H3 hm1, a gift from Dr. G. Schultz (Institut für Pharmakologie, Freie Universität Berlin, Berlin, Germany) and Dr. P. Jones (University of Vermont, Burlington, VT)) were grown in Eagle's minimum essential medium with Earle's salts supplemented with 15% (v/v) heat-inactivated fetal calf serum, 4 mM glutamine, 100 units/ml penicillin, and 100 μg/ml streptomycin in a humidified atmosphere of 5% CO_2 at 37 °C. RBL 2H3 m1 cells were detached from culture plates with SK buffer (125 mM NaCl, 1.5 mM EDTA, 5.6 mM glucose, 10 mM HEPES, pH 7.2); no trypsin was used in order to avoid a partial destruction of membrane receptors. Subconfluent cells were preloaded with anti-TNP IgE (0.3 μg/ml) 12–24 h prior to antigen stimulation experiments. Thereafter, the medium was changed and the cells were treated with toxins for the indicated times and concentrations.

Treatment with Toxins—RBL cells were treated with *C. difficile* toxin B (40 ng/ml, 2–4 h), *C. sordellii* lethal toxin (40 ng/ml, 2–4 h) *C. botulinum* C2 toxin (100 ng/ml C2I and 200 ng/ml C2II 4 h), or *C. limosum* C3 exoenzyme (100 ng/ml C2I and 200 ng/ml C2IN-C3, 4 h) for the indicated times and concentrations. After toxin treatment, cells were washed with the appropriate buffer and used for the assays. To compare properly the effects of toxins, paired experiments were carried out on control and toxin-treated cells that were grown under identical conditions. Additionally, the experiments were repeated with cells of at least two independent passages.

Hexosaminidase Release Assay—Cells were seeded in 96-well culture plates and incubated without or with toxins for the indicated times and concentrations. Hexosaminidase release was determined as described (35). Briefly, the medium was removed, and cells were washed two times with Tyrode buffer (130 mM NaCl, 5 mM KCl, 1.4 mM $CaCl_2$, 1 mM $MgCl_2$, 5.6 mM glucose, 10 mM HEPES, and 0.1% bovine serum albumin, pH 7.4). Incubation at 37 °C with stimuli at the indicated concentrations followed for 1 h. Thereafter aliquots (30 μl) of cells were incubated with 50 μl of 1.3 mg/ml *p*-nitrophenyl-*N*-acetyl-β-D-glucosamide in 0.1 M sodium citrate buffer (pH 4.5) at 37 °C for 1 h. At the end of the incubation, 50 μl of 0.4 M glycine (pH 10.7) stop buffer was added. The total amount of hexosaminidase release was determined using 2% Triton X-100 in Tyrode buffer. Absorbance was measured at 410 nm, referring to 630 nm. The values were expressed as percentage of total amount of hexosaminidase.

Glucosylation and ADP-ribosylation Assay—UDP-[^{14}C]glucosylation was performed as described (36). Cell lysates (about 50 μg of protein) were incubated with 10 μM UDP-[^{14}C]glucose and 1 μg/ml lethal toxin or toxin B for 1 h at 37 °C. For detection of ^{14}C-glucosylated Ras, Ras was immunoprecipitated. Therefore, buffer (final concentrations: 10 mM $MgCl_2$, 150 mM NaCl, 0.1% (w/w) Nonidet P-40, 0.05% (w/w) SDS, 0.5% (w/w) desoxycholate, 40 μg/ml aprotinin, 20 μg/ml leupeptin, 0.1 mM phenylmethylsulfonyl fluoride, 50 mM HEPES, pH 7.4) and anti-Ras beads (15 μl of anti-v-Ha-Ras monoclonal antibody coupled to Sepharose beads, Oncogene Science) were added for 2 h at 4 °C by rotating head-over-head. Beads were collected, washed three times, and boiled with sample buffer. Precipitated proteins were analyzed by SDS-PAGE (15%) and Western blotting. Ras was detected by immunoblot analysis with anti-Ras. Nitrocellulose membranes were analyzed by PhosphorImager SF (Molecular Dynamics).

For ADP-ribosylation, RBL cells were treated with the C3 fusion toxin (100 ng/ml C2IN-C3 and 200 ng/ml C2II) for 4 h at 37 °C. Cells were washed with ice-cold PBS and lysed by addition of ice-cold lysis buffer (2 mM $MgCl_2$, 40 μg/ml aprotinin, 20 μg/ml leupeptin, 80 μg/ml benzamidine, 0.1 mM phenylmethylsulfonyl fluoride, 50 mM HEPES, pH 7.4) and subsequent sonication (five times for 5 s) on ice. ADP-ribosylation was performed as described (37) with 20 μM [^{32}P]NAD and 5 mM $MgCl_2$. Radiolabeled proteins were analyzed by 15% SDS-PAGE and by autoradiography (PhosphorImager SF).

Immunoblotting—RBL cells (10^6) primed with anti-TNP-IgE (0.3 μg/ml) overnight were rinsed twice in PBS and stimulated during 3 min at 37 °C by TNP-OVA (50 ng/ml). After addition of 250 μl of ice-cold lysis buffer (150 mM NaCl, 4 mM EDTA, 1 mM Na_3VO_4, 1% (w/v) desoxycholic acid, 1% (v/v) Nonidet P-40, 0.1% (w/v) SDS, 250 μg/ml *p*-nitrophenyl phosphate, 20 μg/ml aprotinin, 10 mM Tris/HCl, pH 8.0), cell lysates were centrifuged (14,000 × *g*) for 10 min at 4 °C, and the supernatant agitated for 2 h at 4 °C with anti-Rho, anti-Rac2, and anti-Cdc42 from Santa Cruz Biotechnology (Santa Cruz, CA), and anti-Ral monoclonal antibody from Oncogene Science (Uniondale, NY). Protein A/G-agarose was added and the mixture agitated for 1 h. Beads were collected (14,000 × *g*, 5 min), washed twice with ice-cold PBS, mixed, and boiled with sample buffer. Proteins were separated by SDS-PAGE (15%), followed by immunoblotting as described (36). Visualization was performed with a chemiluminescence (ECL) Western blotting detection system (Amersham Pharmacia Biotech, Braunschweig, Germany).

Measurements of $[Ca^{2+}]_i$ in Cell Suspension—RBL cells were detached from culture plates with SK buffer (125 mM NaCl, 1.5 mM EDTA, 5.6 mM glucose, 10 mM HEPES, pH 7.2). Following centrifugation, cells were washed and resuspended in serum-free minimal essential medium and loaded with fura-2 acetoxymethylester (2.5 μM) for 45 min at 37 °C. Then, cells were washed three times with HEPES-buffered salt solution (130 mM NaCl, 5.4 mM KCl, 0.9 mM NaH_2PO_4, 0.8 mM $MgSO_4$, 1.8 mM $CaCl_2$, 10 mM glucose, and 20 mM HEPES, pH 7.4), and cell density was adjusted to 10^6 cells/ml. Experiments were carried out at room temperature in HEPES-buffered salt solution using a Perkin Elmer LS 50B spectrofluorimeter. The fluorescence of cells suspension was examined at an emission wavelength of 510 nm and excitation wavelengths of 340 and 380 nm, respectively. Results are presented as changes in fluorescence ratio 340/380 over time.

Measurements of $[Ca^{2+}]_i$ in Attached Cells—RBL cells were seeded on coverslips, and the intracellular Ca^{2+} was measured at room temperature 2 days later using an cell-imaging system (Till Photonics, Planegg, Germany). In the day of experiments, the cells were incubated in medium containing fura-2 acetoxymethylester (4 μM) for 1 h at room temperature. Subsequently, the culture medium was replaced by a bath solution with a Ca^{2+} concentration of <10 nM (zero Ca_o: 115 mM NaCl, 0.5 mM EGTA, 2 mM $MgCl_2$, 5 mM KCl, 10 mM HEPES, pH 7.2 (NaOH)). The Ca^{2+} concentration in bath was increased to 1 mM (1 mM Ca_o: 115 mM NaCl, 1 mM $CaCl_2$, 2 mM $MgCl_2$, 5 mM KCl, 10 mM HEPES, pH 7.2 (NaOH)) during the fluorescence measurements. Images of 10–25 cells/coverslip were obtained every 3 s at an emission wavelength of 510 nm and excitation wavelengths of 340 and 380 nm, respectively. The fluorescence ratios were calibrated *in vivo* as described previously (38). Experiments were paired by alternating Ca^{2+} measurements in control and toxin-treated coverslips. The data were pooled for statistical analysis and are given as mean ± S.E.

Patch-clamp Techniques—Ionic currents were measured in whole cell mode (39) using an EPC-9 amplifier (HEKA Electronic, Lambrecht, Germany). Whole cell recordings were conducted at room temperature 2–3 days after plating the RBL cells in plastic dishes. For most experiments, depletion of Ca^{2+} stores was induced by cell dialysis through the patch-clamp pipettes (1–2 megohms) with 20 μM IP_3,115 mM CsCl, 4 mM $MgCl_2$, 10 mM EGTA, and 10 mM HEPES (pH 7.2 (CsOH)). When cells were stimulated with the antigen, the dialysate contained no IP_3, instead 300 μM GTP·Na and 2 mM ATP·Mg plus 2 mM $MgCl_2$ were added. The bath solution contained 10 mM $CaCl_2$, 115 mM NaCl, 2 mM $MgCl_2$, 5 mM KCl, and 10 mM HEPES (pH 7.2 (NaOH)). Liquid junction potentials were corrected *a posteriori* (40). The membrane potential was clamped at 0 mV throughout the experiments and whole cell currents were scanned with ramps from +80 mV to −100 mV (0.9 V/s). Since the equilibrium potential for chloride (E_{Cl}) was 0 mV, a current segment of 15 ms was recorded at the holding potential of 0 mV before each ramp was applied. After breaking into whole cell, 12 ramps were delivered every 2 s to obtain reliable leak currents for subsequent leak subtraction. Thereafter, the development of the whole cell currents was followed with ramps delivered every 4 s. Whole cell currents were sampled at 10 kHz and filtered at 1.5 kHz. Series resistance (R_s) and whole cell membrane capacitance (C_m) were electronically compensated (40–50%) before each ramp.

The experiments were scheduled to obtain a similar number of whole cell recordings with control and toxin-treated cells in the same day. Typically, the size (C_m) of the RBL 2H3 hm1 cells corresponds to 10–20 pF and was not changed by the treatment with toxins (controls, 15.3 ± 0.7 pF, n = 19; C2IN-C3, 13.7 ± 1.4 pF, n = 8; toxin B, 15.7 ± 0.8 pF, n = 22; lethal toxin, 16.6 ± 1.2 pF; n = 12). Immediately after breaking into whole cell, an outward current component was usually observed in RBL 2H3 hm1 cells (Fig. 5*A*) but not in RBL-3 cells (data not shown). This outward current was not apparently modified by the treatment with toxins (Fig. 5*B*) and disappeared within the first 4 s of recording. Therefore, the currents obtained at 4–6 s of recording were used for leak subtraction when IP_3 was dialyzed into the cells. In the experi-

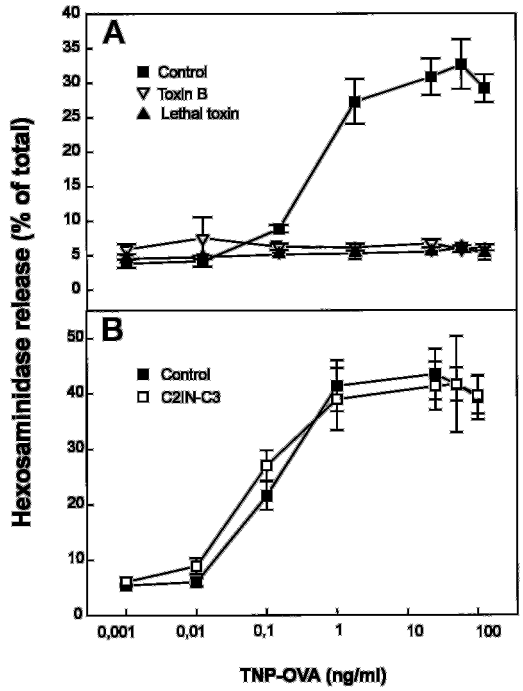

FIG. 1. **Influence of *C. sordellii* lethal toxin, *C. difficile* toxin B, and C3 fusion toxin on hexosaminidase release of RBL cells.** RBL cells were primed by TNP-IgE overnight. Then cells were treated without (■) and with toxin B (▽, 40 ng/ml, *panel A*) and lethal toxin (▲, 40 ng/ml, *panel A*) for 2 h or with C3 fusion toxin (□, 100 ng/ml C2IN-C3 and 200 ng/ml C2II, *panel B*) for 4 h. Thereafter, cells were stimulated by TNP-OVA (*A* and *B*). The release of hexosaminidase was determined as described. Data are given as S.E., $n = 4$.

ments with the antigen, whole cell currents were recorded for 60 s before antigen stimulation and averaged for leak subtraction. Whole cell recordings longer than 60 s showed subthreshold activation of currents probably by depletion of Ca^{2+} stores passively induced by EGTA present in the dialysate. Cells that were not exposed to anti-TNP IgE ($n = 6$) did not respond to antigen stimulation. To obtain current densities, the leak-subtracted currents were normalized to cell size using the corresponding C_m values, except in Fig. 5, which shows raw data. Current densities at −80 mV represent the mean value obtained within a window of 5 mV placed around −80 mV. The holding currents recorded before each ramp were used for calculations of current densities at 0 mV. Only cells with R_s below 7 megohms were pooled for statistical analysis. Data are given as mean ± S.E.

RESULTS

To obtain information about the involvement of Rho GTPases in RBL cell activation, we applied the glucosylating *C. difficile* toxin B and *C. sordellii* lethal toxin, which differ in substrate specificity. Treatment of RBL cells with toxin B (40 ng/ml) or with lethal toxin (40 ng/ml) inhibited the release of hexosaminidase induced by stimulation of the FcεRI (Fig. 1*A*). Using UDP-[^{14}C]glucose and Western blotting, we confirmed that in RBL cells, lethal toxin glucosylates the Rho GTPases Rac and possibly Cdc42 but not Rho. In addition, Ral and Ras (detected by immunoprecipitation, see Fig. 2*B*) were substrates for lethal toxin (Fig. 2, *A* and *B*). As reported recently (36), toxin B modified Rho, Rac, and Cdc42 but not Ras proteins in RBL cell lysates. In contrast to inhibition of secretion by toxin B and lethal toxin, the C3 fusion toxin C2IN-C3 (27), that selectively and completely ADP-ribosylated Rho (Fig. 2*C*) but not Rac and Cdc42 had no effect on secretion induced by TNP-OVA (Fig. 1*B*). Thus, these findings confirmed that Rac/Cdc42 but not Rho are essential for secretion in RBL cells.

Since the increase in $[Ca^{2+}]_i$ is a prerequisite for secretion in RBL cells, we studied the effects of the lethal toxin and toxin B on the Ca^{2+} mobilization induced by TNP-OVA in RBL cells. Because treatment of RBL cells with clostridial toxins affect the cytoskeleton possibly interfering with the adherence of cells, we first tested the effects of the toxins in suspension. Under these conditions and in the presence of extracellular Ca^{2+}, toxin B and lethal toxin blocked the Ca^{2+} mobilization (Fig. 3*A*). Next, we tested the effects of C3 exoenzyme, which selectively modifies RhoA, -B, and -C but not Rac or Cdc42. Because cell accessibility of C3 exoenzyme is rather poor, we used the fusion toxin C2IN-C3, which is able to enter cells readily and shows the same substrate specificity as C3 (27). As shown in Fig. 3*B*, C2IN-C3 did not affect TNP-OVA-induced Ca^{2+} mobilization. The glucosylating cytotoxins affect the actin cytoskeleton in many cell types including RBL cells (23); therefore, we studied the role of the redistribution of the actin cytoskeleton on the Ca^{2+} response using *C. botulinum* C2 toxin, which ADP-ribosylates actin and induces depolymerization of actin filaments (33). C2 toxin did not inhibit but rather increased the late phase of the Ca^{2+} transients induced by TNP-OVA (Fig. 3*C*).

The effects of the toxin B and lethal toxin shown in Fig. 3 can be explained by inhibition of one or several steps in the intracellular signaling cascade initiated by stimulation of the FcεRI receptor and leading to mobilization of intracellular Ca^{2+}. To test a possible effect of toxin B and lethal toxin on the signaling cascade between release of Ca^{2+} from intracellular stores and activation of capacitative Ca^{2+} influx, we used thapsigargin, a potent inhibitor of Ca^{2+} ATPases involved in Ca^{2+} storage, that is frequently used to induce opening of store-regulated Ca^{2+} channels in a receptor-independent manner (41). Moreover, thapsigargin and antigen reportedly activate the same store-regulated Ca^{2+} influx in RBL cells (42). As shown in Fig. 4*A*, toxin B and lethal toxin inhibited the thapsigargin-induced Ca^{2+} mobilization. Again, thapsigargin-induced Ca^{2+} mobilization was not inhibited by C2 toxin (Fig. 4*B*). This finding supported the view that toxin B and lethal toxin likely affect the capacitative Ca^{2+} influx underlying the Ca^{2+} mobilization induced by FcεRI receptor stimulation.

Therefore, we studied the effects of the toxins in patch clamp experiments to detect a possible inhibition of I_{CRAC}. The depletion of Ca^{2+} stores was induced in a receptor-independent manner by cell dialysis with IP_3 (Fig. 5). Typically, the current-voltage relationships changed very rapidly reflecting the increase of inward currents both in control and toxin-treated cells and steady-state current levels were attained after 60 s after beginning of the dialysis of IP_3 (Fig. 5*A*). No difference in the time course of current activation was observed between control and toxin treated cells, except that the steady-state currents were consistently smaller in cells treated with toxin B (Fig. 5*B*). To analyze this difference, the current amplitudes were normalized to cell size (Fig. 6). In control and toxin-treated cells (Fig. 6*A*), the whole cell currents showed an inward rectification and reversed at strong positive potentials (data not shown), as described for I_{CRAC} in various cell systems (43). When the whole cell currents of cells treated with toxin B and lethal toxin were scaled by a factor of 1.4–1.7, the scaled currents superimposed on whole cell currents measured in paired control cells (Fig. 6*A*, *inset*). By contrast, I_{CRAC} was not much changed by treatment with C2IN-C3 (Fig. 6*A*). When paired experiments were compared, the current densities of cells treated with toxin B and lethal toxin were 46% and 40% smaller than control current densities at −80 mV, respectively (Fig. 6*B*). At −80 mV, the current densities of cells treated with C2IN-C3 were not significantly smaller than controls but significantly larger than current densities of cells treated with toxin B and lethal toxin ($p < 0.01$). Since the equilibrium potential for chloride was 0 mV in the present experimental conditions, we compared also current densities at 0 mV in order

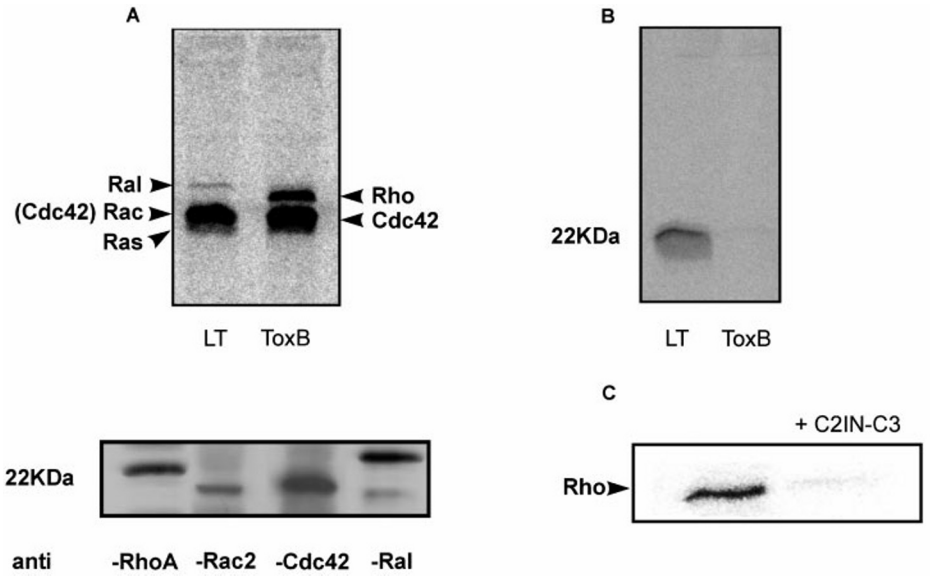

FIG. 2. **Modification of low molecular mass GTPases by *C. sordellii* lethal toxin, *C. difficile* toxin B, and C3 fusion toxin.** *A*, lysates from RBL cells were glucosylated by lethal toxin (*LT*, 1 μg/ml) or toxin B (*ToxB*, 1 μg/ml) in the presence of 10 μM UDP-[^{14}C]glucose for 1 h at 37 °C. After incubation the proteins were separated by 15% SDS-PAGE. PhosphorImager data of the gel are shown (*upper panel*). Single protein bands were identified by Western blot analysis with anti-RhoA, anti-Rac2, anti-Cdc42, and anti-Ral-antibodies (*lower panel*). *B*, lysates from RBL cells were ^{14}C-glucosylated by lethal toxin or toxin B as described above. Anti-Ras beads were added for 2 h at 4 °C. After agitating head-over-head, beads were collected, washed three times, and boiled with sample buffer. Proteins were separated by 15% SDS-PAGE, and [^{14}C]incorporation was evaluated with the PhosphorImager. *C*, effectiveness of treatment of RBL cells with C3 fusion toxin. The C3 fusion toxin consists of the active fusion protein C2IN-C3 and the binding component C2II. RBL cells were treated with C2IN-C3 (100 ng/ml) and C2II (200 ng/ml) for 4 h. Thereafter, cells were washed and lysed. The cell lysate was ADP-ribosylated in the presence of [^{32}P]NAD (20 μM) and C3 exoenzyme (1 μg/ml). Radioactively labeled proteins were identified by SDS-PAGE and autoradiography (PhosphorImager data are shown).

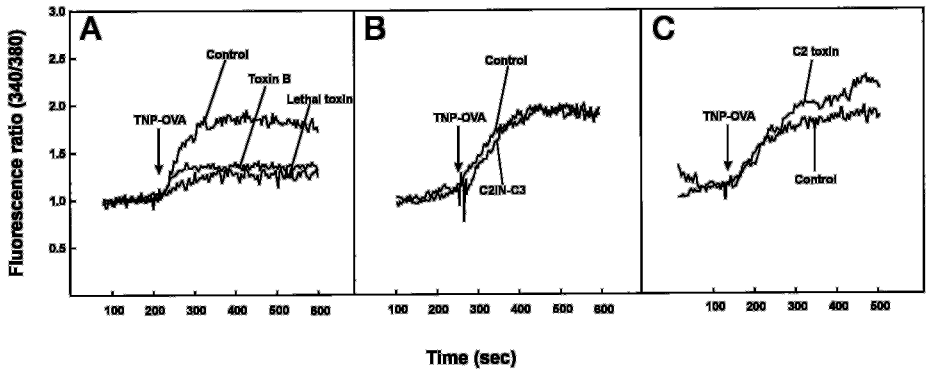

FIG. 3. **Influences of toxins on Ca^{2+} responses of RBL cells primed with anti-TNP-IgE.** Cells were treated with toxin B (40 ng/ml), lethal toxin (40 ng/ml) for 2 h (*A*), C3 fusion toxin (100 ng/ml C2IN-C3 and 200 ng/ml C2II) for 4 h (*B*), and C2 toxin (100 ng/ml C2I and 200 ng/ml C2II) for 4 h (*C*). Control represents paired experiments with cells that were not treated with toxins. Cells were stimulated by TNP-OVA (50 ng/ml).

to rule out a possible contamination of Cl^- currents. Although the amplitude of steady-state currents at 0 mV is small in RBL cells (5–10 pA), the current densities of cells treated with toxin B and lethal toxin but not with C21N-C3 were consistently smaller than current densities of control cells (control, -0.41 ± 0.23 pA/pF, $n = 17$; C2IN-C3, -0.35 ± 0.21 pA/pF, $n = 8$; toxin B, -0.25 ± 0.17 pA/pF, $n = 18$; lethal toxin, -0.21 ± 0.14 pA/pF, $n = 9$). Same inhibition by the glucosylating toxins was observed when I_{CRAC} was activated by stimulation of the FcεRI receptor with TNP-OVA in cells primed with anti-TNP-IgE (Fig. 7) instead of depletion of Ca^{2+} stores induced by dialysis of IP_3 (Figs. 5 and 6). These results strongly indicate both toxin B and lethal toxin but not C2IN-C3 inhibited I_{CRAC} in RBL cells, probably by interfering at steps of the signaling cascade between depletion of Ca^{2+} stores and activation of CRAC channels in the plasma membrane of RBL cells. Furthermore, since in contrast to the effects of the clostridial cytotoxins, the fusion toxin C2IN-C3 did not reduce whole cell currents, it is likely that Rac and Cdc42 but not Rho are involved in the activation of I_{CRAC} following stimulation of the FcεRI receptor.

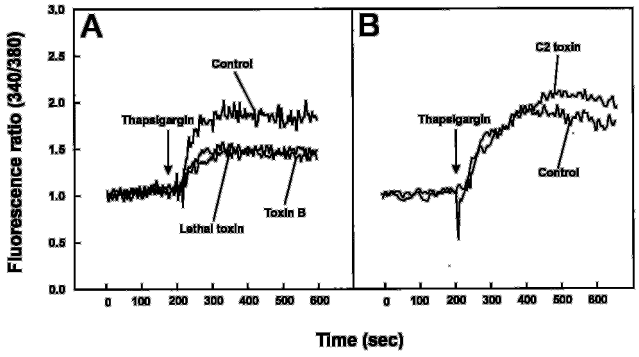

FIG. 4. **Influences of toxin B, lethal toxin, and C2 toxin on Ca^{2+} response induced by thapsigargin in RBL cells.** Cells were treated with toxin B (40 ng/ml), lethal toxin (40 ng/ml) for 2 h (*A*) and C2 toxin (100 ng/ml C2I and 200 ng/ml C2II) for 4 h (*B*). Control represents paired experiments with non-treated cells. Cells were stimulated with thapsigargin (100 nM).

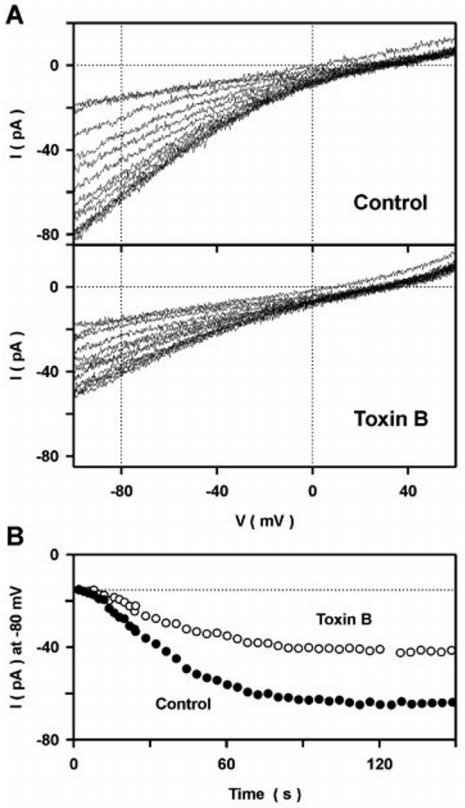

FIG. 5. **Activation of I_{CRAC} in RBL cells treated with toxin B.** Depletion of intracellular Ca^{2+} stores was induced by dialysis of 20 μM IP_3. To illustrate the inhibition of I_{CRAC} by toxin B, current recordings obtained in the same day with cells of approximately identical size (control, 15 pF; toxin B, 16 pF) were selected. The original traces (*A*) represent the first 12 non-subtracted currents recorded every 4 s after beginning of IP_3 dialysis. Superimposed are the steady-state currents recorded at 120 s. The time course of I_{CRAC} activation (*B*) is depicted for current amplitudes at −80 mV.

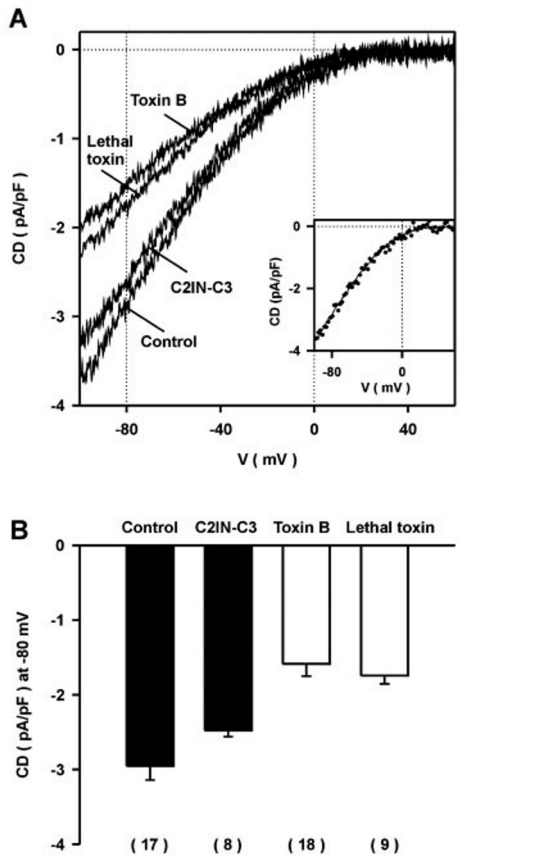

FIG. 6. **Effects of toxin B, lethal toxin, and C2IN-C3 on I_{CRAC}.** The activation of whole cell currents was induced by cell dialysis with 20 μM IP_3 and the steady-state currents obtained at 120–240 s were leak-subtracted and expressed as current density (*CD*). The representative current traces (*A*) were recorded in a control RBL cell and in cells treated with toxin B, lethal toxin and C2IN-C3. The *inset* illustrates the steady-state current of the cell treated with toxin B (●) scaled up by a factor of 1.6 and superimposed on the smoothed current of the control cell (*continuous line*). The current densities at −80 mV were pooled for statistical analysis (*B*). Current densities of cells treated with toxin B and lethal toxin are significantly smaller than the current density of control cells ($p < 0.001$), respectively. No statistically significant difference between current densities of control and C2IN-C3 treated cells was found. The number of experiments is given in the parenthesis.

The Ca^{2+} signals of RBL cells are normally characterized by a biphasic response. The initial transient phase due largely to a Ca^{2+} release from IP_3 is usually followed by a sustained plateau due to capacitative Ca^{2+} entry through CRAC channels (43, 44). Since the experiments shown in Fig. 5–7 indicated that toxin B and lethal toxin inhibited the activation of I_{CRAC}, we tested whether the capacitative Ca^{2+} entry is modified by toxin B. In the absence of extracellular Ca^{2+}, stimulation of the FcεRI receptor of adherent RBL cells by TNP-OVA caused a small and transient increase in $[Ca^{2+}]_i$ due to release of Ca^{2+} from intracellular stores (Fig. 8*A*). After increasing the extracellular Ca^{2+} concentration to 1 mM, the capacitative Ca^{2+} entry was observed in control and toxin-treated cells (Fig. 8*A*). Treatment of RBL cells with toxin B did not effect the release of Ca^{2+} from intracellular stores observed in the absence of extracellular Ca^{2+} but inhibited the capacitative Ca^{2+} entry in the presence of 1 mM $[Ca^{2+}]_o$ by about 52% (Fig. 8*B*). These results support the view that toxin B and lethal toxin reduce the Ca^{2+} mobilization induced by activation of the FcεRI receptor mainly by inhibiting I_{CRAC} and consequently the capacitative Ca^{2+} entry in RBL cells.

DISCUSSION

Several studies have demonstrated that Rho GTPases are involved in FcεRI-mediated activation of RBL cells and mast cells (22, 45, 46). Secretion from permeabilized mast cells were increased by dominant active Rac and Rho proteins (20). Gomperts and co-workers suggested Rac and Cdc42 as candidates for "G_E," a GTP-binding protein, mediating exocytosis in cells of hematopoietic origin (21). A role of small GTPases of the Rho family in RBL and mast cell activation was supported by recent findings that toxin B, which glucosylates and inactivates Rho GTPases, completely blocks secretion in these cells (36). However, the precise role of Rho GTPases in activation of RBL cells is still a matter of debate. Here we studied the effects of clostridial cytotoxins that inactivate Rho GTPases on the Ca^{2+} mobilization in RBL 2H3 hm1 cells. Our findings indicate that Rho GTPases play an essential role in the Ca^{2+} response of high affinity IgE receptors. Toxin B as well as lethal toxin inhibited not only the TNP-OVA-induced secretion but also the increase in $[Ca^{2+}]_i$. The effects of the toxins were much stronger in the presence of extracellular Ca^{2+} suggesting an action on Ca^{2+} entry rather than on release from internal Ca^{2+} stores. Toxin B modifies all Rho GTPases known including Rho, Rac, and Cdc42 subtypes (29); lethal toxin inactivates Rac and, to a minor extent, Cdc42 but not Rho. In addition, Ras subfamily proteins like Ras and Ral are modified by lethal toxin (30). Thus, our data indicate that Rac (or Cdc42) but not Rho is involved in the toxins' effects on Ca^{2+} mobilization. This notion is supported by the findings that the fusion toxin C2IN-C3, which selectively inactivates RhoA, -B, and -C, was without effect on secretion and Ca^{2+} mobilization (27, 47). Rho GTPases

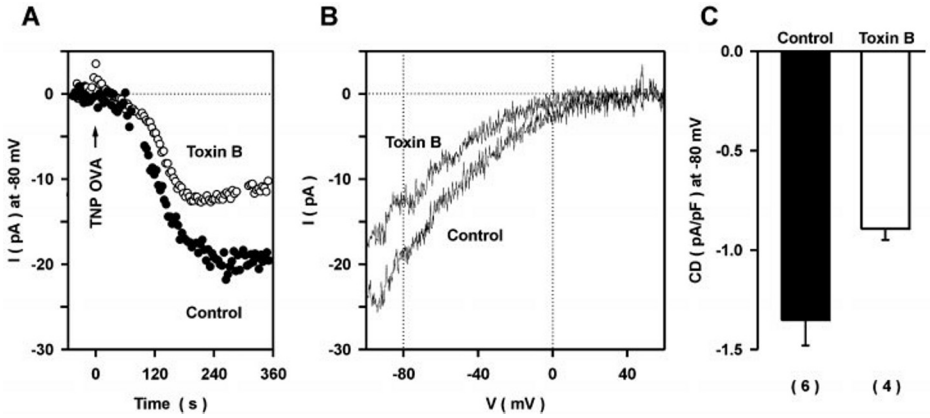

FIG. 7. **Inhibition of the antigen activation of I_{CRAC} by toxin B.** Following a base-line recording of 60 s, TNP-OVA (50 ng/ml) was applied to RBL cells primed with anti TNP-IgE. Two representative experiments with cells of approximately identical size (control, 15 pF; toxin B, 14 pF) are illustrated. Whole cell currents were leak-subtracted. The time course of I_{CRAC} at −80 mV (*A*) showed a delay of more than 60 s before the current amplitude increased to steady-state levels. The steady-state currents (*B*) were obtained at 240 s. The current densities (*CD*) of cells treated with toxin B were 35% smaller ($p < 0.01$) than current densities of control cells at −80 mV (*C*).

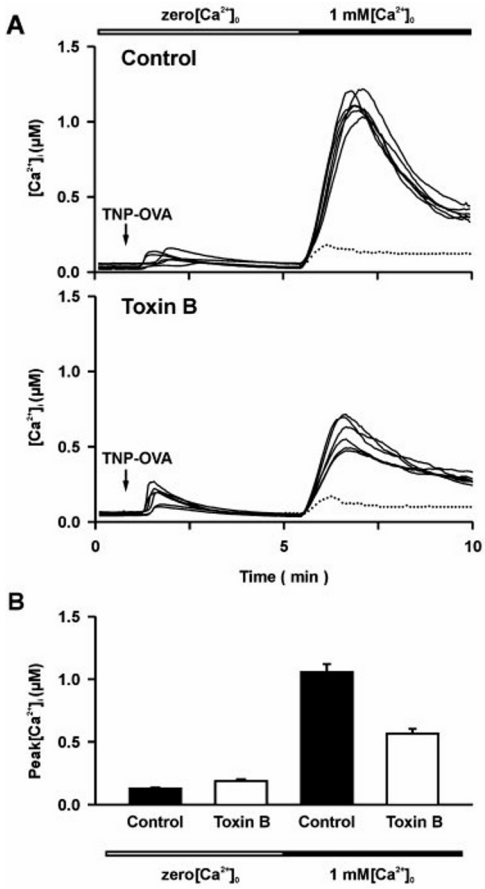

FIG. 8. **Capacitative Ca^{2+} entry in RBL cells treated with toxin B.** RBL cells that were previously primed with anti-TNP-IgE were exposed to a Ca^{2+}-free solution (zero $[Ca^{2+}]_o$). Subsequently, TNP-OVA (50 ng/ml) was applied and the extracellular Ca^{2+} concentration was increased to 1 mM (1 mM $[Ca^{2+}]_o$). *A*, time course of the intracellular Ca^{2+} concentration ($[Ca^{2+}]_i$) in 6 representative control and toxin B-treated cells. The *dotted line* represents the average response to the change from 0 to 1 mM $[Ca^{2+}]_o$ in cells (control, $n = 7$; toxin B, $n = 12$) that were not stimulated with TNP-OVA. *B*, peak values of $[Ca^{2+}]_i$ in zero $[Ca^{2+}]_o$ after stimulation with TNP-OVA and in 1 mM $[Ca^{2+}]_o$. Peak values in 1 mM $[Ca^{2+}]_o$ were 52% smaller in cells treated with toxin B ($n = 68$) than in control cells ($n = 57$).

are master regulators of the actin cytoskeleton. Therefore, it was tested whether redistribution of the actin cytoskeleton plays a major role in toxin-caused inhibition of the Ca^{2+} response by FcεRI activation. Because C2 toxin, which causes depolymerization of actin filaments (33), showed no inhibition but rather an increase in Ca^{2+} mobilization, we conclude that the role of the Rho GTPases in the Ca^{2+} response is largely independent of the actin cytoskeleton.

Importantly, we observed that the clostridial cytotoxins also inhibited thapsigargin-induced increase in $[Ca^{2+}]_i$. Thapsigargin blocks sarco-endoplasmic reticulum Ca^{2+}-ATPases (41) and thereby promote influx of Ca^{2+} in RBL cells by passive depletion of IP_3-sensitive Ca^{2+} stores (42, 48). Thus, our data suggested that the toxin-sensitive step, *e.g.* the site of action of Rac/Cdc42 in regulation of Ca^{2+} mobilization, may be located downstream of IP_3 production. To further substantiate this hypothesis, we performed whole cell patch-clamp experiments to characterize the CRAC channel suggested to be involved in ligand-regulated Ca^{2+} entry in RBL cells. In line with the findings on the Ca^{2+} mobilization determined with the Fura method, we observed inhibition of the TNP-OVA-induced increase in I_{CRAC} by the clostridial cytotoxins. Moreover, IP_3-induced activation of the CRAC channel was inhibited by the Rac/Cdc42-modifying toxins, suggesting a role of the GTPases in this process.

So far the precise regulatory functions of Rac/Cdc42 in Ca^{2+} responses are unclear. At least three models have been proposed for signaling capacitative Ca^{2+} entry (7, 49). First, it was suggested that a diffusible signaling factor (calcium influx factor) is generated and released from the endoplasmic reticulum (50). Second, conformational coupling model was proposed in which the endoplasmic reticulum IP_3 receptor directly interacts with the Ca^{2+} channel in the plasma membrane (51). Finally, recent studies suggest a secretion-like coupling leading to fusion of vesicles containing Ca^{2+} channels with the plasma membrane, thereby allowing Ca^{2+} entry (52, 53).

Rho proteins including Rho, Rac, and Cdc42 have been reported to regulate endocytic and/or exocytic events (54–56). Moreover, these GTPases have been suggested to be involved in Ca^{2+} signaling by various receptors. Recent studies on the Fcγ receptor signaling indicate that Rho GTPases participate in the Ca^{2+} response in J774 macrophages (57). In these cells, Rho itself appears to be essential, because microinjection of C3 exoenzyme blocked the Fcγ receptor-mediated Ca^{2+} response. As reported in the present article, however, in RBL cells, ADP-ribosylation of Rho by the fusion toxin C2IN-C3 neither effected Ca^{2+} signaling nor secretion. In HeLa cells, transfection of dominant negative N17Rac blocked Ca^{2+} influx stimulated by epidermal growth factor, suggesting an essential role of Rac

in Ca^{2+} response mediated by the receptor tyrosine kinase (58). Thus, it appears that the involvement of Rho GTPases in Ca^{2+} mobilization largely depends on the cell type studied.

In summary, we show that Rac/Cdc42 but not Rho are not only essential for late secretory events of RBL cell activation but also control specifically the Ca^{2+} response induced by the high affinity IgE receptor (FcεRI).

Acknowledgment—We thank Dr. V. Flockerzi for helpful critical reading of the manuscript.

REFERENCES

1. Beaven, M. A., and Metzger, H. (1993) *Immunol. Today* **14,** 222–226
2. Hutchcroft, J. E., Geahlen, R. L., Deanin, G. G., and Oliver, J. M. (1992) *Proc. Natl. Acad. Sci. U. S. A.* **89,** 9107–9111
3. Minoguchi, K., Benhamou, M., Swaim, W. D., Kawakami, Y., Kawakami, T., and Siraganian, R. P. (1994) *J. Biol. Chem.* **269,** 16902–16908
4. Beaven, M. A., and Kassessinoff, T. (1997) in *IgE Receptor (FcεRI) Function in Mast Cells and Basophils* (Hamawy, M. M., ed) pp. 55–73, R. G. Landes Co., Austin, TX
5. Kinet, J.-P. (1999) *Annu. Rev. Immunol.* **17,** 931–972
6. Penner, R., Matthews, G., and Neher, E. (1988) *Nature* **334,** 499–504
7. Barritt, G. J. (1999) *Biochem. J.* **337,** 153–169
8. Parekh, A. B., and Penner, R. (1997) *Physiol. Rev.* **77,** 901–930
9. Fasolato, C., Hoth, M., and Penner, R. (1996) *J. Biol. Chem.* **268,** 20737–20740
10. Hall, A. (1998) *Science* **279,** 509–514
11. Ridley, A. J., and Hall, A. (1992) *Cell* **70,** 389–399
12. Ridley, A. J., Paterson, H. F., Johnston, C. L., Diekmann, D., and Hall, A. (1992) *Cell* **70,** 401–410
13. Nobes, C. D., and Hall, A. (1995) *Cell* **81,** 53–62
14. Malcolm, K. C., Ross, A. H., Qiu, R.-G., Symons, M., and Exton, J. H. (1994) *J. Biol. Chem.* **269,** 25951–25954
15. Illenberger, D., Schwald, F., Pimmer, D., Binder, W., Maier, G., Dietrich, A., and Gierschik, P. (1998) *EMBO J.* **17,** 6241–6249
16. Zhang, J., King, W. G., Dillon, S., Hall, A., Feig, L., and Rittenhouse, S. E. (1993) *J. Biol. Chem.* **268,** 22251–22254
17. Hawkins, P. T., Eguinoa, A., Qiu, R.-G., Stokoe, D., Cooke, F. T., Walters, R., Wennström, S., Claesson-Welsh, L., Evans, T., Symons, M., and Stephens, L. (1995) *Curr. Biol.* **5,** 393–403
18. Chong, L. D., Traynor-Kaplan, A., Bokoch, G. M., and Schwartz, M. A. (1994) *Cell* **79,** 507–513
19. Van Aelst, L., and D'Souza-Schorey, C. (1997) *Genes Dev.* **11,** 2295–2322
20. Price, L. S., Norman, J. C., Ridley, A. J., and Koffer, A. (1995) *Curr. Biol.* **5,** 68–73
21. Brown, A. M., O'Sullivan, A. J., and Gomperts, B. D. (1998) *Mol. Biol. Cell* **9,** 1053–1063
22. Guillemot, J.-C., Montcourrier, P., Vivier, E., Davoust, J., and Chavrier, P. (1997) *J. Cell Sci.* **110,** 2215–2225
23. Aktories, K. (1997) *Trends Microbiol.* **5,** 282–288
24. Aktories, K., Rösener, S., Blaschke, U., and Chhatwal, G. S. (1988) *Eur. J. Biochem.* **172,** 445–450
25. Paterson, H. F., Self, A. J., Garrett, M. D., Just, I., Aktories, K., and Hall, A. (1990) *J. Cell Biol.* **111,** 1001–1007
26. Aktories, K., Braun, U., Rösener, S., Just, I., and Hall, A. (1989) *Biochem. Biophys. Res. Commun.* **158,** 209–213
27. Barth, H., Hofmann, F., Olenik, C., Just, I., and Aktories, K. (1998) *Infect. Immun.* **66,** 1364–1369
28. Aktories, K., and Just, I. (1995) *Trends Cell Biol.* **5,** 441–443
29. Just, I., Selzer, J., Wilm, M., Von Eichel-Streiber, C., Mann, M., and Aktories, K. (1995) *Nature* **375,** 500–503
30. Just, I., Selzer, J., Hofmann, F., Green, G. A., and Aktories, K. (1996) *J. Biol. Chem.* **271,** 10149–10153
31. Popoff, M. R., Chaves, O. E., Lemichez, E., Von Eichel-Streiber, C., Thelestam, M., Chardin, P., Cussac, D., Chavrier, P., Flatau, G., Giry, M., Gunzburg, J., and Boquet, P. (1996) *J. Biol. Chem.* **271,** 10217–10224
32. Von Eichel-Streiber, C., Harperath, U., Bosse, D., and Hadding, U. (1987) *Microb. Pathogen.* **2,** 307–318
33. Aktories, K., Bärmann, M., Ohishi, I., Tsuyama, S., Jakobs, K. H., and Habermann, E. (1986) *Nature* **322,** 390–392
34. Jones, S. V. P., Choi, O. H., and Beaven, M. A. (1991) *FEBS Lett.* **289,** 47–50
35. Ozawa, K., Szallasi, Z., Kazanietz, M. G., Blumberg, P. M., Mischak, H., Mushinski, J. F., and Beaven, M. A. (1993) *J. Biol. Chem.* **268,** 1749–1756
36. Prepens, U., Just, I., Von Eichel-Streiber, C., and Aktories, K. (1996) *J. Biol. Chem.* **271,** 7324–7329
37. Aktories, K., and Just, I. (1995) *Methods Enzymol.* **256,** 184–195
38. Philipp, S., Hambrecht, J., Braslavski, L., Schroth, G., Freichel, M., Murakami, M., Cavalié, A., and Flockerzi, V. (1998) *EMBO J.* **17,** 4247–4248
39. Hamill, O. P., Marty, A., Neher, E., Sakmann, B., and Sigworth, F. J. (1981) *Pflügers Arch.* **391,** 85–100
40. Neher, E. (1992) *Methods Enzymol.* **207,** 123–131
41. Treiman, M., Caspersen, C., and Christensen, S. B. (1998) *Trends Pharmacol. Sci.* **19,** 131–135
42. Ali, H., Maeyama, K., Sagi-Eisenberg, R., and Beaven, M. A. (1994) *Biochem. J.* **304,** 431–440
43. Hoth, M., and Penner, R. (1992) *Nature* **355,** 353–356
44. Choi, O. H., Lee, J.-H., Kassessinoff, T., Cunha-Melo, J. R., Jones, S. V. P., and Beaven, M. A. (1993) *J. Immunol.* **151,** 5586–5595
45. Norman, J. C., Price, L. S., Ridley, A. J., and Koffer, A. (1996) *Mol. Biol. Cell* **7,** 1429–1442
46. Norman, J. C., Price, L. S., Ridley, A. J., Hall, A., and Koffer, A. (1994) *J. Cell Biol.* **126,** 1005–1016
47. Just, I., Mohr, C., Schallehn, G., Menard, L., Didsbury, J. R., Vandekerckhove, J., van Damme, J., and Aktories, K. (1992) *J. Biol. Chem.* **267,** 10274–10280
48. Zhang, L., and McCloskey, M. A. (1995) *J. Physiol.* **483,** 59–66
49. Putney, J. W., Jr. (1999) *Cell* **99,** 5–8
50. Rzigalinski, B. A., Willoughby, K. A., Hoffman, S. W., Falck, J. R., and Ellis, J. (1999) *J. Biol. Chem.* **274,** 175–182
51. Kiselyov, K., Xu, X., Mozhayeva, G., Kuo, T., Pessah, I., Mignery, G., Zhu, X., Birnbaumer, L., and Muallem, S. (1998) *Nature* **396,** 478–482
52. Yao, Y., Ferrer-Montiel, A. V., Montal, M., and Tsien, R. Y. (1999) *Cell* **98,** 475–485
53. Gill, D. L., and van Rossum, D. B. (1999) *Cell* **98,** 487–499
54. Lamaze, C., Chuang, T. H., Terlecky, L. J., Bokoch, G. M., and Schmid, S. L. (1996) *Nature* **382,** 177–179
55. Schmalzing, G., Richter, H. P., Hansen, A., Schwarz, W., Just, I., and Aktories, K. (1995) *J. Cell Biol.* **130,** 1319–1332
56. Kroschewski, R., Hall, A., and Mellman, I. (1999) *Nat. Cell Biol.* **1,** 8–13
57. Hackam, D. J., Rotstein, O. D., Schreiber, A., Zhang, W., and Grinstein, S. (1997) *J. Exp. Med.* **186,** 955–966
58. Peppelenbosch, M. P., Tertoolen, L. G. J., De Vries-Smits, A. M. M., Qiu, R.-G., M'Rabet, L., Symons, M. H., de Laat, S. W., and Bos, J. L. (1996) *J. Biol. Chem.* **271,** 7883–7886